

## Optical Control of Thermocapillary Effects in Complex Nanofluids

Yuval Lamhot,<sup>1</sup> Assaf Barak,<sup>1</sup> Carmel Rotschild,<sup>1</sup> Mordechai Segev,<sup>1</sup> Meirav Saraf,<sup>2</sup> Efrat Lifshitz,<sup>2</sup> Abraham Marmur,<sup>3</sup> Ramy El-Ganainy,<sup>4</sup> and Demetrios N. Christodoulides<sup>4</sup>

<sup>1</sup>*Physics Department, Technion, Haifa 32000, Israel*

<sup>2</sup>*Chemistry Department, Technion, Haifa 32000, Israel*

<sup>3</sup>*Chemical Engineering Department, Technion, Haifa 32000, Israel*

<sup>4</sup>*CREOL—College of Optics, University of Central Florida, Florida 32816, USA*

(Received 29 July 2009; published 29 December 2009)

We study the strong coupling of light and nanoparticle suspensions and their surface tension effect in capillaries. We show experimentally and theoretically that increasing the intensity of a narrow laser beam passing through a capillary far away from the surface results in a significant decrease in the fluid level. The underlying mechanism relies on light-induced redistribution of nanoparticles in the bulk and the surface of the fluid, facilitating continuous optical control over the surface position. The experiments manifest optical control from afar over properties of fluid surfaces.

DOI: 10.1103/PhysRevLett.103.264503

PACS numbers: 47.55.dm, 42.70.-a, 47.55.dr, 47.57.-s

The field of optofluidics initiated a breakthrough in integration of microfluidic systems with optics. Optofluidics relies on the utilization of the optical properties of materials and liquids to perform various functions upon illumination, combined with the ability to modify optical properties of devices by manipulating the fluids [1]. Optofluidics is expected to play an important role in a variety of areas [2]. There are many examples of miniaturized systems with networks of fluidic channels, valves, pumps and other means of fluidic encapsulation and manipulation, in which light monitors the fluids. One promising direction has to do with colloidal dispersions of particles, specifically of the nanometric scale [3]. The use of dispersions gives rise to novel properties, depending on the kind of the colloidal particles, their innate size and their surface physics. The optical features of such suspensions (absorption, fluorescence, etc.) can be altered by varying the parameters of the particles (concentration, diameter, refractive index). In general, colloidal particles are made of a variety of materials (dielectrics, metals, and semiconductors) and are used in optical tweezers, fluorescence detection in biology, and more [3]. The distinct nature of optofluidic systems gives rise to new hydrodynamic and hydrostatic effects and enhanced surface activity [4]. Furthermore, colloidal dispersions are greatly influenced by particle distribution due to unique optical, thermal, and equilibrium characteristics of such systems [5–7].

Recent studies demonstrated light manipulation of fluid surfaces by direct illumination of the interface, via momentum transfer [8] or heating [9]. Here, we study the interaction between light and suspensions of dielectric nanoparticles, focusing on optical control over surface tension effects. We show that passing a narrow laser beam through a vertical capillary containing a complex fluid leads to a significant change in the fluid height, even when the beam is far from the surface. The interaction between light and the complex fluid exhibits highly non-

local effects: the diameter of the beam is 1000 times smaller than its distance to the interface, yet increasing the beam intensity causes a very large height drop. Each time the intensity is varied the system reaches a new hydrostatic state, giving rise to a new fluid height. The hydrostatic state of the system manifests a balance between light-induced particle distribution and light-induced thermal changes in the fluid. We model the effects and show that light absorption by the nanoparticles forms a thermal gradient, which redistributes the particles through thermophoresis, and consequently modifies surface tension and changes the fluid height in the capillary. We find good agreement between theory and experiments with no free parameters. The vision is to develop new avenues for optically manipulating the surface tension of liquids.

Experimentally, we use a 5  $\mu\text{m}$  FWHM beam of vacuum wavelength of 514 nm. Our fluid includes Oleic-Acid-covered CdTe and CdSe nanoparticles suspended in liquid octadecene. The particles have 2–4 nm diameters, and their initial concentration is  $\sim 10^{16} \text{ cm}^{-3}$ . A liquid reservoir is filled with the colloidal solution, and a Pyrex capillary ( $\sim 500 \mu\text{m}$  diameter) is placed inside it [Fig. 1(a)]. The reservoir is positioned such that the beam waist is inside the capillary, at an initial distance below the meniscus,  $\Delta X_0$ . We monitor the beam by observing the fluorescence of the nanoparticles, and measure the meniscus height drop,  $\Delta H$ , as a function of  $\Delta X_0$  [Figs. 1(b) and 1(c)].

In our system, the optical interaction with the complex fluids occurs via absorption in the nanoparticles, giving rise to thermal effects. It is therefore essential to carry out a control experiment, with the same capillary heated by a heat source: a metal wire. Before heating [Fig. 1(d)], the fluid is uniform in color. Once the heating begins, the hue of the fluid fades in the vicinity of the heating wire [Fig. 1(e)], and the solution has the clarity of pure octadecene, with no particles in it. Further away from the wire, the color reappears, until it returns completely  $\sim 2 \text{ mm}$

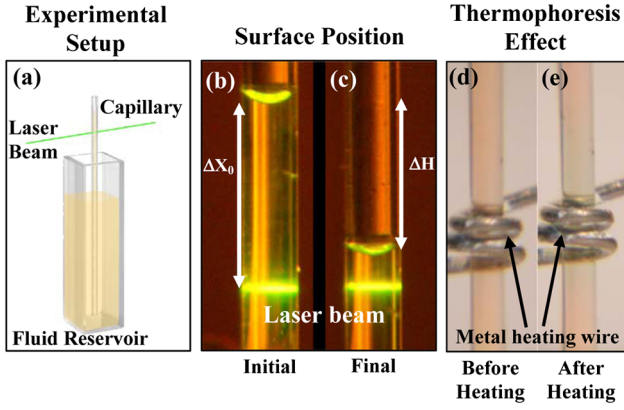


FIG. 1 (color online). (a) Experimental setup. (b),(c) The capillary with nanoparticle fluid illuminated by a laser beam before (b) and after (c) the height of the surface changes. The bright yellow line is due to the fluorescence nature of the nanoparticles at the vicinity of the beam. (d),(e) A heating wire around a capillary filled with a CdTe solution at room temperature before (d) and after (e) heating. The solution turns clear where the temperature is higher, due to the thermophobic nanoparticles.

away from the heat source. This phenomenon is due to thermophoresis (Soret effect), in which particles drift due to temperature gradient [7]. Examining the fluid height in this control experiment reaffirms a known result [10]: when the fluid height begins to drop, it drops all the way to the heat source (the hot wire). Thus, when the heat source is thermal, the fluid height in the capillary, at temporal steady state, is predetermined by the position of the heat source, with no intermediate heights. As we show next, when the process is driven by light, the fluid height is continuously controlled by the light intensity, and all intermediate states are reachable.

We now turn to light-induced surface tension experiments, where a laser beam passes through the capillary at  $\Delta X_0$  below the surface and induces a height change  $\Delta H$  of the fluid-air interface [Fig. 1(c)]. In contrast to earlier work [4,9,10], we control the meniscus height optically, from afar, and tune the height continuously by varying the beam power. The particles absorb light and transfer the heat to the liquid, thereby creating a thermal profile in it, which is affected by heat conduction and convection in and around the capillary. The light-induced temperature distribution changes the nanoparticle concentration via thermophoresis, producing a new concentration profile in the capillary. For a given  $\Delta X_0$ , the final level of the fluid is uniquely determined by the beam power: each power level produces a stable steady-state position. This interaction between light-induced heat diffusion and light-induced thermophoresis brings forth the ability to have continuous control over surface tension effects using a remote light beam.

Figure 2 shows our results on light-induced control over fluid height in a capillary, carried out with various nanoparticle solutions. In all cases, we see a continuous range of steady-state positions, depending on the beam power [Figs. 2(a)–2(c)]. Increasing the power causes the height

to drop, until it reaches a new stable position. At steady state, the height change,  $\Delta H$ , always increases (the fluid drops) as power is increased, until it saturates at high power [Fig. 2(d)]. Also,  $\Delta H$  increases when the initial distance between the beam and the surface,  $\Delta X_0$ , is decreased [Figs. 2(a)–2(c)]. In all measurements the stabilization time of the height in its new light-induced position is several seconds. The effect is fully reversible: once the illumination is blocked, the surface returns to its initial height. We emphasize the difference from the control experiment, where the heat source is the metal wire, and the fluid level (at steady state) is predetermined by the heat source, and no intermediate states are possible. The ability to control the fluid height is unique to the optics experiment: it relies on the fact that the heat source (the light-absorbing nanoparticles) is dynamic, and its strength depends on the thermal gradient, due to thermophoresis.

In surface tension effects, the contact angle  $\theta$  plays an important role. To isolate its role, we measure  $\theta$  with and without illumination, and find that  $\theta$  does not change from its initial value of  $22^\circ \pm 5^\circ$  for all our beam power values and  $\Delta X_0$ . This is supported by studies showing that organic fluid interfaces with  $\cos(\theta) \cong 1$  have a constant angle over a wide range of temperatures [6]. In those studies, fluids with similar compositions, surface tension, and contact angle (Dodecene, Decene, etc.), have a small negative value of  $d\theta/dT$ . Therefore, changes in  $\theta$  are minute, and  $\cos(\theta)$  remains practically constant for a wide range of temperatures. Consequently, we take a fixed  $\theta$  in our model.

We model the system in steady state, when the fluid height depends on the optical power and distance of the beam from the surface. Under such conditions, the heat diffusion equation reads

$$-k \frac{\partial^2 T}{\partial x^2} = \varepsilon C(x) I_{\text{beam}}(x) - \kappa(T - T_a), \quad (1)$$

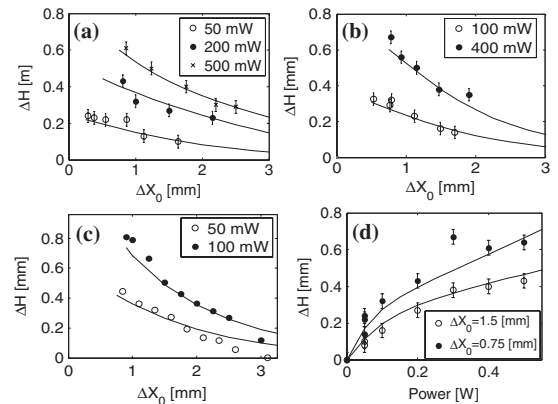


FIG. 2. (a),(b) Steady-state height change  $\Delta H$  in a solution with 3.5 nm CdTe particles, vs initial distance between the beam and the surface,  $\Delta X_0$ , for various beam powers. (c) Same as (a) with 2.5 nm CdSe particles. (d) Steady-state height change in a solution with 3.5 nm CdTe particles vs beam power, for  $\Delta X_0 = 0.75, 1.5$  mm. Solid lines represent theoretical results, with no fitting parameters.

where  $T(x)$  is the temperature as a function of position [ $x = 0$  indicates the beam position],  $k$  is heat conduction constant,  $\varepsilon$  is the optical absorption coefficient for the nanoparticles, and  $C(x)$  is the nanoparticles' concentration.  $I_{\text{beam}}$  is the intensity of the laser beam. The last term represents heat convection, due to natural convection of air around the capillary. The term is based on Newton's law of cooling and depends on  $T_a$ , the ambient temperature of the surrounding, and on  $\kappa$  which is the decay rate. From Eq. (1) we calculate  $T(x)$ , and with  $T(x)$  we determine the light-induced distribution of particles, using the thermophoresis equation (at low  $C(x)$  and at steady state) [7]

$$\nabla C = -C(x)S_T(T)\nabla T \quad (2)$$

where  $S_T$  is the Soret coefficient. The temperature and concentration profiles affect surface tension. Using the van der Waals–Guggenheim equation, the thermal dependence of the surface tension is

$$\sigma = \sigma_0 \left(1 - \frac{T(x)}{T_c}\right)^n, \quad (3)$$

where  $\sigma$  is the surface tension of the fluid,  $\sigma_0$  is a constant typical of the fluid,  $T_c$  is the fluid critical temperature, and  $n$  is an exponent whose value is 11/9 for many organic liquids. We use the Szyszkowski equation to describe  $\sigma_{\text{complex}}$ , the surface tension of the complex fluid, as

$$\sigma_{\text{complex}} = \sigma(1 - b \ln[1 + aC(x)]) \quad (4)$$

where  $b$  is the constant obtained from the partial area the particles acquire on the interface, and  $a$  is the interface adsorption coefficient. Equations (3) and (4) give the surface tension of the complex fluid, which determines the height of the fluid through the capillary rise equation

$$H = \frac{2\sigma_{\text{interface}} \cos(\theta)}{\rho g R}, \quad (5)$$

where  $H$  is the height of the fluid meniscus above the reservoir,  $\sigma_{\text{interface}}$  is the liquid-to-air surface tension,  $\rho$  is the fluid density,  $g$  is the gravitational constant and  $R$  is the radius of the capillary. The height difference  $\Delta H$  is the difference between the original height (due to the original surface tension) and the final height the system reaches after the surface tension changes. The fluid density is roughly constant for a wide temperature range. This is evident experimentally since heating and expanding of the fluid would increase the capillary rise, opposite to our findings. Furthermore, illuminating or heating far away from the interface causes no change in the fluid level, implying that the fluid density variations are negligible.

The steady-state solution of these equations, yielding the final position of the surface  $\Delta H = X - \Delta X_0$ , occurs when the solution is self-consistent. We seek this solution, given the beam power and  $\Delta X_0$ , in the following manner. We first obtain  $T(x)$  from Eq. (1). With  $T(x)$  we find  $C(x)$  [Eq. (2)], and calculate the surface tension and the new meniscus position. After determining  $T(x)$ ,  $C(x)$  and the capillary

height [via Eqs. (3)–(5)], we return to the beginning of the procedure and solve Eq. (1) again using the new  $C(x)$  and the relative position of the surface from the previous iteration. We iterate until the values of  $\Delta H$  and the profiles converge, e.g., when the difference in  $\Delta H$  between iterations is  $< 0.1 \mu\text{m}$ . We use our experimental parameters (capillary diameter, etc.), along with material constants we measure directly or use tabulated values. For CdTe,  $\sigma_0 = 52 \text{ mN/m}$ ,  $b = 3 \times 10^{-3} \text{ N/m}$ , and  $a = 5.3 \times 10^{20} \text{ m}^{-3}$ , which we measure by the pendant drop method. For the absorbance coefficient we measure  $\varepsilon \sim 2 \times 10^{-21} \text{ m}^2$ . The main difference in the values of the CdSe nanoparticles is their absorbance, which is almost double that of CdTe. For octadecene,  $T_c = 740 \text{ K}$ ,  $\rho = 0.8 \times 10^3 \text{ kg/m}^3$ , and the system heat conductance  $k = 0.7 \text{ W/m} \cdot \text{K}$  [11]. The typical values and thermal behavior of the Soret coefficient for nanoparticles are taken from [7]. For the convective term in Eq. (1), we take  $T_a = 23 \text{ }^\circ\text{C}$ . Because of the geometry of the system,  $\kappa$  is calculated by taking  $h$  (the convective heat transfer coefficient) and dividing it by  $R/2$  where  $R = 250 \mu\text{m}$ .  $h$  is calculated using an average Nusselt number ( $\overline{\text{Nu}}$ ) with proper correlations for a natural convection of the cylindrical system [11]. The calculated value of  $\overline{\text{Nu}}$  is  $\sim 1.9$ , corresponding to  $h = 57 \text{ W/m}^2\text{K}$  and  $\kappa = 4.56 \times 10^5 \text{ W/m}^3\text{K}$ . We calculate the temperature decay length ( $\sqrt{k/\kappa}$ )  $\sim 1.2 \text{ mm}$ . We calculate the Gr number in the capillary, to rule out internal convection flows, and find  $\text{Gr} \sim 0.05$ , meaning that viscous forces counteract the buoyancy forces in the fluid, and heat flow inside the fluid is only via the conduction term. Calculating Bo yields  $\sim 10^{-2}$ ; hence, changes in the meniscus height are greatly influenced by changes in the surface tension and not from variations in fluid density.

We plot the predictions of our model on the experimental figures (solid lines in Fig. 2). The model predictions are in good agreement with the experimental results, with no fitting parameters. As Figs. 2(a) and 2(c) show, our model is relevant for different types of particles. In fact, the model can be used for any fluid system with thermophoretic particles. Clearly, our model confirms our main finding: the steady-state surface height in our system yields a continuum of values, in contrast with earlier work [4] where only one stable position was possible. This is explained as follows. In the absence of thermophoresis and light-induced redistribution of the absorbing particles [4–7], the temperature rise at the surface (due to the absorption) decreases surface tension, and lowers the fluid height. In that case there is no mechanism to stop the height drop; hence, the surface temperature continues to rise as the surface level drops until the meniscus reaches the beam and stops there. This thermocapillary effect has only one stable position—the hot spot itself. In contrast, in our experiments, the light-induced thermophoresis combines competing mechanisms which yield a continuous range of steady-state positions. On one hand, increasing the light intensity generates heat, which diffuses to the surface,

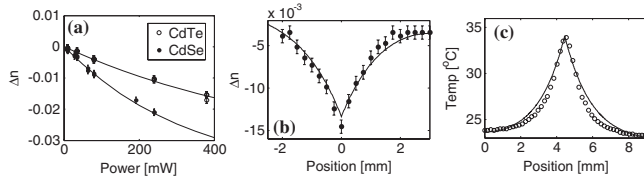


FIG. 3. (a) Maximum refractive index change ( $\Delta n$  at the beam vicinity) vs beam power, for CdTe and CdSe solutions. (b) Profile of the refractive index change in a CdTe particle solution, inside the capillary (beam position set as zero). (c) Measured (circles) and calculated (solid line) temperature profiles in the capillary for CdSe solution ( $\Delta X_0 = 4.5$  mm,  $I_{\text{beam}} = 120$  mW, surface position set at zero). The temperature at the surface is higher than room temperature.

accumulates there (because the air above is an insulator), and reduces surface tension. On the other hand, thermophoresis causes particles to migrate away from the surface [Eq. (4)]; hence, the decline in surface tension slows down. Also, the nanoparticles migrating away from the beam, thereby decrease absorption, and less heat is transferred to the fluid [Eq. (1)]. These combined effects, especially the latter, are the reason for the continuous range of positions, which are controllable optically from far away from the surface.

Our model also predicts the temperature profile  $T(x)$  and the particle distribution  $C(x)$  in the fluid. We find that the refractive index change,  $\Delta n(x)$ , arising from thermal effects in the liquid, is stronger than the index change resulting from variations in particle concentration. Thus,  $\Delta n(x)$  provides another means of mapping  $T(x)$ . To measure  $\Delta n(x)$ , we construct a Mach-Zender interferometer, measuring the phase change for a weak plane-wave propagating through the capillary (perpendicular to the beam controlling the surface height). We measure the maxima of  $\Delta n$  vs beam power [Fig. 3(a)], at the vicinity of the beam. As the measurements and the theory demonstrate, the CdSe nanoparticles solution shows higher  $\Delta n$  than the CdTe solution. This is due to the higher absorption of the CdSe particles, which correlates with higher temperature changes in the capillary. As predicted by theory [solid lines in Fig. 3(a)], the change in the maxima of  $\Delta n$  decreases for increasing power. This is a result of thermophoresis, causing migration of more particles away from the beam as the power increases, decreasing the ability to absorb light and generate heat. This is also the reason for the saturation in Fig. 2(d), where  $\Delta H$  decreases as beam power increases. Figure 3(b) shows  $\Delta n$  vs height in the capillary, obtained from the interference pattern. The profile  $T(x)$  is taken with a thermal camera [Fig. 3(c)]. Comparing the measured  $T(x)$  and  $\Delta n(x)$  profiles to those predicted by the model shows good agreement. The figure also shows that the temperature at the fluid-air interface is slightly higher than the ambient room temperature or the temperature at the capillary base. Since the particle concentration in the reservoir is roughly the initial concentration, we conclude

that the particles concentration at the top of the capillary is lower than the initial concentration. As demonstrated by Fig. 3(c), there is a clear long-range thermal effect of the illumination on the complex fluid system.

The experiments and the model show how an optical beam continuously tunes the fluid level, which uniquely depends on the beam intensity. The light alters both the temperature distribution and the particle distribution. The steady-state behavior manifests balance between the various mechanisms underlying the surface tension, hence controlling the capillary rise. The experiments show strong dependence on the beam power, which our model predicts with excellent accuracy.

In conclusion, we demonstrated light control over surface tension, due to coupling of thermocapillary effect and light-induced nanoparticle redistribution. We showed that a focused laser beam can accurately control the fluid level in a capillary over a continuous range of heights. These effects suggest several applications and raise many appealing aspects. For example, using light to induce surface tension effects can control Marangoni flow. In addition, using thermophoretic particles, the dynamics of the fluid can also affect the propagation of the light beam inducing the flow, in a symbiotic fashion.

This work was supported by an Advanced Grant from the European Research Council (ERC) and by the Israel-USA Binational Science Foundation (BSF).

- 
- [1] D. Psaltis, S.R. Quake, and C. Yang, *Nature (London)* **442**, 381 (2006).
  - [2] U. Levy *et al.*, *Microfluid Nanofluid* **4**, 97 (2008).
  - [3] S.K. Lee *et al.*, *Microfluid Nanofluid* **4**, 129 (2008).
  - [4] P.Y. Chiou, Z. Chang, and M.C. Wu, *J. MEMS* **17**, 133 (2008); E. Verneuil *et al.*, *Langmuir* **25**, 5127 (2009); M. Dietzel and D. Poulikakos, *Phys. Fluids* **17**, 102106 (2005); V. Pratap, N. Moumen, and R.S. Subramanian, *Langmuir* **24**, 5185 (2008).
  - [5] P. Lavi and A. Marmor, *J. Colloid Interface Sci.* **230**, 107 (2000).
  - [6] A.W. Neumann, *Adv. Colloid Interface Sci.* **4**, 105 (1974).
  - [7] R. Piazza and A. Parola, *J. Phys. Condens. Matter* **20**, 153102 (2008); S. Duhr and D. Braun, *Phys. Rev. Lett.* **96**, 168301 (2006); M. Braibanti, D. Vigolo, and R. Piazza, *ibid.* **100**, 108303 (2008).
  - [8] R.D. Schroll *et al.*, *Phys. Rev. Lett.* **98**, 133601 (2007).
  - [9] G.L. Liu *et al.*, *Nature Mater.* **5**, 27 (2006).
  - [10] P.S. Glockner and G.F. Naterer, *J. Micromech. Microeng.* **15**, 2216 (2005); K. Ichimura *et al.*, *Science* **288**, 1624 (2000); M.W.J. Prins *et al.*, *Science* **291**, 277 (2001).
  - [11] F.P. Incropera *et al.*, *Fundamentals of Heat and Mass Transfer* (John Wiley & Sons Inc., Hoboken, NJ, 2006), 6th ed.; I. Owczarek and K. Blaze, *J. Phys. Chem. Ref. Data* **32**, 1411 (2003); *CRC Handbook of Chemistry and Physics* (Taylor & Francis, London, 2010), 90th ed.; C.L. Yaws, *Handbook of Thermal Conductivity* (Gulf Publishing Com., Houston, TX, 1995).